Symmetry-Dependent Exciton-Phonon Coupling in 2D and Bulk MoS_2 Observed by Resonance Raman Scattering

Bruno R. Carvalho,* Leandro M. Malard, Juliana M. Alves, Cristiano Fantini, and Marcos A. Pimenta†
Departamento de Física, Universidade Federal de Minas Gerais, Belo Horizonte, Minas Gerais 30123-970, Brazil
(Received 17 September 2014; published 2 April 2015)

This work describes a resonance Raman study performed on samples with one, two, and three layers ($1L$, $2L$, $3L$), and bulk MoS_2, using more than 30 different laser excitation lines covering the visible range, and focusing on the intensity of the two most pronounced features of the Raman scattering spectrum of MoS_2 (E^1_{2g} and A_{1g} bands). The Raman excitation profiles of these bands were obtained experimentally, and it is found that the A_{1g} feature is enhanced when the excitation laser is in resonance with A and B excitons of MoS_2, while the E^1_{2g} feature is shown to be enhanced when the excitation laser is close to 2.7 eV. We show from the symmetry analysis of the exciton-phonon interaction that the mode responsible for the E^1_{2g} resonance is identified as the high energy C exciton recently predicted [D. Y. Qiu, F. H. da Jornada, and S. G. Louie, Phys. Rev. Lett. 111, 216805 (2013)].

DOI: 10.1103/PhysRevLett.114.136403 PACS numbers: 71.35.-y, 63.20.kd, 63.22.Np, 78.30.-j

Excitonic effects are expected to be very strong and influence the optical properties of 2D materials, such as the MoS_2-type transition metal dichalcogenides (TMDs), giving rise to the rich physics reported in the literature [1–3]. Resonance Raman spectroscopy is a very useful tool to study excitonic transitions and exciton-phonon interactions in semiconductors [4] and, in this work, we present a resonance Raman study of $1L$, $2L$, $3L$, and bulk MoS_2 samples. Our results show that the A_{1g} feature is enhanced when the excitation laser is in resonance with the A and B excitons of MoS_2, while the E^1_{2g} feature is shown to be enhanced when the excitation laser is close to 2.7 eV, in a region of the optical spectrum of MoS_2 that possesses a diversity of excitonic states that cannot be distinguished at room temperature [1]. We present a symmetry analysis that shows that the in-plane E^1_{2g} phonon couples preferentially with the predicted high energy exciton state near the Γ point, called the C exciton [1]. Our results show that phonons of MoS_2 with different symmetries are enhanced by different types of excitons, and provide experimental values for the dependence of the exciton energies and lifetimes on the number of layers.

Sekine *et al.* [5] were the first to report a resonance Raman study of TMD compounds and measured the Raman excitation profile (REP) of the A_{1g} and E^1_{2g} modes of bulk $2H$-MoS_2, -WS_2, -$MoSe_2$ and -WSe_2, using many different laser lines in the range of laser energies 1.6–2.8 eV. In the case of MoS_2 and WS_2, only the A_{1g} mode was observed to resonate with the A and B excitons, but both A_{1g} and E^1_{2g} peaks were enhanced at higher energies. This high energy resonance was observed to be broad and it was attributed to the transition between the high density of states in the valence and conduction bands. Sourisseau *et al.* [6] have also measured the REP of the A_{1g} and E^1_{2g} bands in bulk WS_2 in the range of the A and B excitons, and obtained results similar to those reported by Sekine *et al.* [5]. Frey *et al.* [7] showed using dynamics calculation that the electronic structure is modulated when applying the A_{1g}-mode displacement for the material, but not significantly affected by the E^1_{2g}-mode displacements. These previous works show that the A_{1g} phonon couples preferentially with the A and B excitons, but report similar behavior for the A_{1g} and E^1_{2g} modes at higher laser excitation energies. We will show below that, contrarily to the previous resonance Raman results [5,6], the A_{1g} and E^1_{2g} modes exhibit different resonant Raman behavior at higher laser energies.

With the recent possibility of producing two-dimensional (2D) TMD samples, a number of Raman studies of few-layer MoS_2 have been reported. It has been observed that the Raman spectrum is significantly dependent on the laser excitation energy [8–13]. Scheuschner *et al.* [14] measured the REP of the A_{1g} phonon mode of $1L$ and $2L$ MoS_2 in the range of laser energies of the A and B excitons (1.75–2.05 eV) [14], and observed that the amplitude of the REP associated with the B transition is larger than the A REP amplitude. It was also reported in this work [14] that the amplitudes of the REPs are larger in bilayer than in monolayer MoS_2, suggesting that the electron-phonon coupling decreases with a decreasing number of atomic layers. The enhancement of the A_{1g} mode under resonance with the A and B excitons was also observed in recent Raman studies of $1L$ and few-layer MoS_2 [15,16], but detailed results using many different laser lines of higher energies were not reported in the previous resonance Raman studies of 2D MoS_2.

In this Letter we present a resonant Raman spectroscopy study of MoS_2 samples of $1L$, $2L$, $3L$, and bulk using up to 30 excitation energies in the visible range. Our measurements allowed us to obtain separately the REP of the A_{1g} and E^1_{2g} Raman bands. Our results confirm previous conclusions that the A_{1g} band resonates preferentially with

the A and B excitons, but shows, for the first time, that the E^1_{2g} band exhibits a strong and sharp resonance around 2.7 eV, which is ascribed to the coupling of this specific phonon with an exciton with different k-space characteristics (C exciton), recently predicted [1].

All details about the samples and the Raman experiments, including the different laser sources and a polarization analysis, are presented in the Supplemental Material [17]. In addition, a group theory analysis and the assignment of the Raman modes are also presented in the Supplemental Material [17].

Figure 1 shows the Raman spectra of $1L$, $2L$, $3L$, and bulk MoS_2 obtained with many different laser excitation energies, in the spectral range 300–500 cm^{-1}. The peaks around 387 and 410 cm^{-1} correspond, respectively, to the in-plane E^1_{2g} and the out-of-plane A_{1g} phonons (for notation simplicity, we will use the irreducible representations of bulk MoS_2) [26,27]. We can see in Fig. 1 that the relative intensities of these modes are strongly dependent on the excitation energy. The A_{1g} mode is more intense than the E^1_{2g} for laser energies below 2.5 eV and above 2.8 eV, but there is a clear inversion in the intensities of these peaks, for all investigated samples, in the range 2.6–2.7 eV. This result was not reported so far in the literature.

In order to understand this effect in more detail, Fig. 2 shows the Raman excitation profile of the A_{1g} and E^1_{2g} phonon modes for (a) $1L$, (b) $2L$, (c) $3L$, and (d) bulk MoS_2 samples. The intensities of the MoS_2 Raman peaks were normalized by the intensity of the Si Raman peak of the substrate, considering its excitation energy dependence as reported by Renucci *et al.* [28]. There is a correction in the relative intensities of the MoS_2 and Si peaks due to multiple optical interferences in the SiO_2 layer. However, as discussed in the Supplemental Material [17], this correction does not affect our main results and conclusions.

The REP of the bulk sample, depicted in Fig. 2(d), shows two maxima for the A_{1g} phonon mode (black triangles) around 1.9 and 2.1 eV, which are associated with the A and B excitonic transitions. The intensities of these two maxima decrease in the case of few-layer MoS_2, and are very weak for the monolayer sample, as shown in Fig. 2(a). This result is in agreement with a previous resonance Raman study of this phonon in the region of the A and B excitons [14]. We can also see in Fig. 2 that the E^1_{2g} phonon mode is strongly enhanced for all samples at higher laser excitation energies, around 2.7 eV.

The REP of the A_{1g} and E^1_{2g} modes shown in Fig. 2 were fitted by the expression for the Raman intensity as a function of the laser energy E_L derived by a third-order time dependent perturbation theory, and given by [4]:

$$I(E_L) = K\left|\frac{\langle f|H_{e-r}|b\rangle\langle b|H_{e-\mathrm{ph}}|a\rangle\langle a|H_{e-r}|i\rangle}{(E_L - E_{\mathrm{ex}} - i\gamma)(E_L - E_{\mathrm{ph}} - E_{\mathrm{ex}} - i\gamma)}\right|^2, \quad (1)$$

where $\langle f|H_{e-r}|b\rangle$, $\langle b|H_{e-\mathrm{ph}}|a\rangle$, and $\langle a|H_{e-r}|i\rangle$ are the matrix elements associated with the electron-radiation, exciton-phonon, and electron-radiation interactions, respectively, and E_{ex} is the energy of the intermediate excitonic state (A, B, or C). The damping constant γ is related to the finite lifetime τ of the intermediate states, and E_{ph} is the corresponding phonon energy. The red curves in

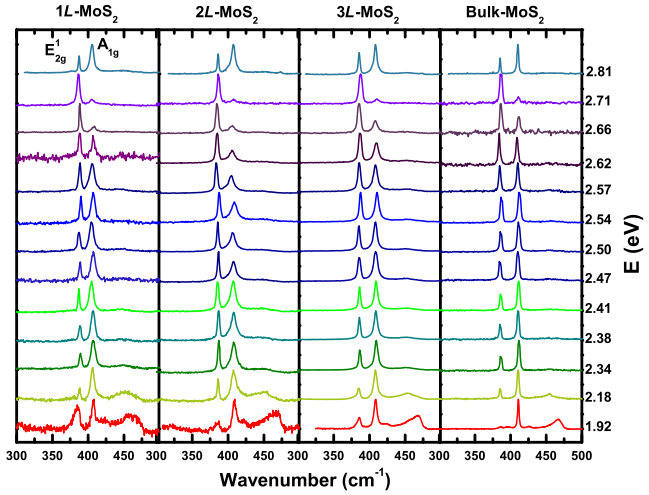

FIG. 1 (color online). Raman spectra of MoS_2 samples with a different number of layers, and recorded with the different laser excitation energies shown in the right side. Panels from left to right correspond, respectively, to 1, 2, and 3 layers, and bulk samples.

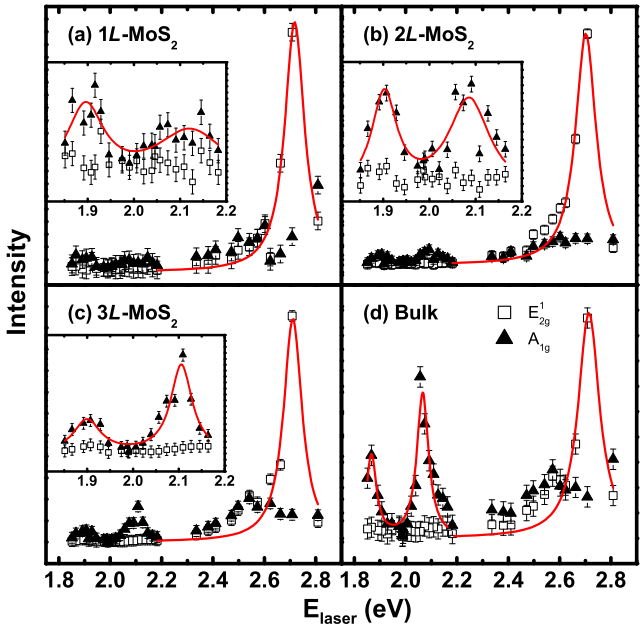

FIG. 2 (color online). Raman excitation profiles of the E^1_{2g} (open squares) and A_{1g} (solid triangles) Raman peaks in (a) monolayer, (b) bilayer, (c) trilayer, and (d) bulk MoS_2 samples. The insets show a zoom-in of the data in the range of 1.8–2.2 eV. The red curves represent the fitting of the experimental data by the expression given in Eq. (1).

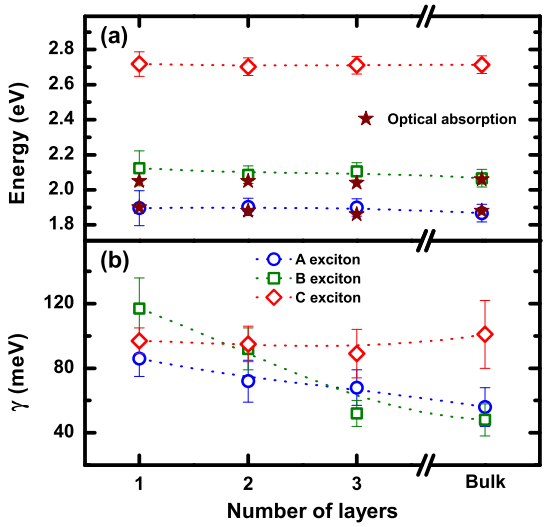

FIG. 3 (color online). (a) Energies and (b) damping constants of the A, B, and C excitons for the samples with a different number of layers. Red stars represent optical absorption values from Ref. [29] for $1L$, $2L$, and $3L$ and from Ref. [30] for bulk.

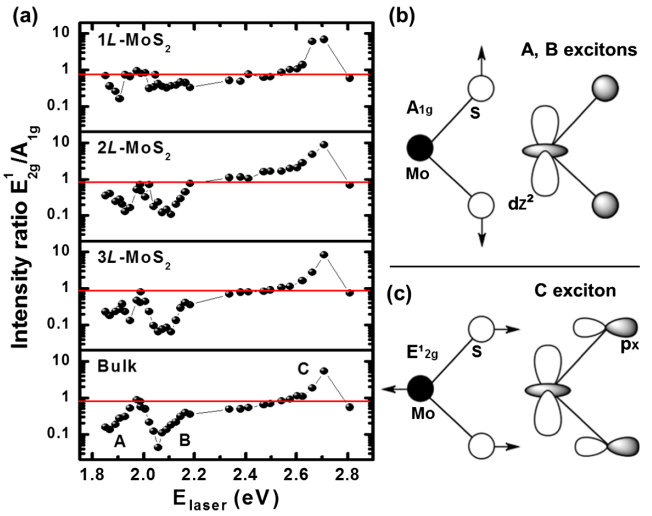

FIG. 4 (color online). (a) Ratio of the intensities of the E^1_{2g} and A_{1g} Raman bands, plotted in a logarithmic scale. (b) Atomic displacements of the A_{1g} phonon mode and electronic orbitals of the A and B excitons. (c) Atomic displacements of the E^1_{2g} phonon mode and electronic orbitals of the C exciton.

Fig. 2 correspond to the best fit of the experimental data, and Figs. 3(a) and 3(b) show, respectively, the energy and damping constant values, as a function of the number of layers, obtained from the fitting of Fig. 2 by Eq. (1).

Let us now discuss the observed enhancement of the E^1_{2g} mode at 2.7 eV. The optical spectrum of bulk $2H$-MoS_2 was measured more than 40 years ago [31,32] and, besides the sharp peaks ascribed to the A and B excitons, a broad band was also observed between 2.5 and 3.3 eV. This band was shown to exhibit two maxima around 2.76 and 3.18 eV, denominated respectively as C and D peaks. In these pioneer works, the C and D peaks were interpreted as optical transitions between high density of states regions at the K and M points of the 2D Brillouin zone. This high energy broad band was also observed in the optical spectra of atomically thin MoS_2 samples [29], and it was observed that its position blueshifts with a decreasing number of layers.

In a resonance Raman study of bulk $2H$-MoS_2 crystal, Sekine *et al.* [5] showed that the A_{1g} mode REP exhibits two sharp peaks at 1.93 and 2.15 eV, and a broad peak at 2.61 eV. The sharp peaks were attributed to the A and B excitons and the broad peak to the direct band-to-band transition [32]. The E^1_{2g} peak was also observed to be enhanced in the region of the broad peak at 2.61 eV. Our results, presented in Fig. 2, agree with previous resonance Raman studies of MoS_2 in the range of the A and B excitons, but clearly show that the E^1_{2g} mode is specially enhanced at higher laser energies. In order to show this effect more clearly, Fig. 4(a) plots the ratio between the intensities of the E^1_{2g} and A_{1g} bands in a logarithmic scale, as a function of the laser excitation energy, for the different samples studied in this work. Points below (above) the horizontal red line correspond to enhancements of the A_{1g} (E^1_{2g}) mode.

In a recent first-principle calculation of the optical response of monolayer MoS_2 [1], Qiu *et al.* showed that the broad band in the optical spectra between 2.5 and 3.3 eV has contributions of different types of excitons and excitonic states, which cannot be spectrally resolved at room temperature. Besides the excited states of the A and B excitons (A' and B'), the existence of a bound excitonic state with novel k-space characteristics, called the C exciton state, was also predicted.

Let us discuss if the enhancement of the E^1_{2g} phonon mode is due to the band-to-band transition, as proposed many years ago by Sekine *et al.* [5], or by a high energy excitonic transition, predicted recently by Qiu *et al.* [1]. First, notice in Fig. 2 that the enhancement of the E^1_{2g} mode around 2.7 eV is stronger and sharper than the enhancement of the A_{1g} mode around 1.9 and 2.1 eV, which are demonstrated to be associated with the A and B exciton states. When the intermediate state in a Raman process is excitonic, the Raman cross section is enhanced more strongly than when the intermediate states correspond to band-to-band transitions [33–35]. Moreover, the Raman excitation profile of the E^1_{2g} phonon around 2.7 eV (see Fig. 2) is much sharper than the broad band in the optical spectra of MoS_2. This result suggests that, among many excitonic states that contribute to the broad band in the optical spectra in the range of 2.5–3.3 eV, the E^1_{2g} mode is selectively enhanced by a specific excitonic state. This selective enhancement is related to the exciton-phonon matrix element, given by the middle term in the numerator of Eq. (1), which depends on the phonon and the exciton symmetries.

This distinct exciton-phonon coupling can be explained considering the symmetries of the A_{1g} and E^1_{2g} phonons and of the orbitals associated with the A, B, and C excitons. According to Ref. [1], the A and B excitons reflect the Mo d_{z^2} orbitals of the states in the lowest MoS_2 conduction band, and the exciton wave function is azimuthally symmetric, with the orbitals pointing along the z direction [see Fig. 4(b)]. On the other hand, the C exciton originates from a sixfold degenerate state made from transitions between the highest valence band and the first three lowest conduction bands near, but not directly at, the Γ point of the Brillouin zone [1]. When this exciton is plotted in real space, the electron has both Mo d_{z^2} and S p_x and p_y, with more S character near the hole. The representation of the C exciton orbitals is shown in Fig. 4(c). The A_{1g} mode involves out-of-plane vibration of S atoms and, therefore, it is expected to modulate the d_{z^2} orbitals more strongly than the E^1_{2g} in-plane mode. The situation is the opposite for the C exciton due to the presence of the in-plane p_x and p_y orbitals shown in Fig. 4(c). In this case, the in-plane movements of the S atoms modulate the electronic cloud and, therefore, one can expect a stronger exciton-phonon coupling for the E^1_{2g} mode with the C exciton.

The symmetry-dependent exciton-phonon coupling can be also discussed using group theory arguments. For both few-layer and bulk MoS_2, the d_{z^2} orbitals belong the totally symmetric irreducible representation (A'_1, A_{1g} and A_{1g} for odd few-layer, even few-layer and bulk, respectively), whereas the p_x and p_y orbitals belong to a two-dimensional irreducible representation (E', E_g, and E_{2g} for odd few layer, even few layer and bulk, respectively). Therefore, the d_{z^2} orbitals couple with the totally symmetric out-of-plane phonon [26,27], and the A_{1g} mode is enhanced by the A and B excitons. On the other hand, the two-dimensional $p_{x,y}$ orbitals of the C excitonic state couple with the two-dimensional in-plane E^1_{2g} phonon [26,27], explaining why it is enhanced by resonance with the C exciton. Notice that the C exciton is not exactly at the Γ point, but at sixfold points within the interior of the BZ that do not exhibit inversion symmetry. Therefore, the exciton-phonon coupling between the C exciton and the E^1_{2g} mode is indeed allowed by group theory.

Figure 3(a) shows that the values of the exciton energies obtained from our resonance Raman results do not depend significantly on the number of layers, within our experimental uncertainty. Figure 3(a) also shows the A and B exciton energy values obtained from optical absorption experiments [29,30], which are in a good accordance with our resonance Raman results. It is interesting to observe that the difference between the A and B exciton energies, which is related to the spin-orbit splitting [36], is practically the same for few-layer and bulk MoS_2 (0.23, 0.18, 0.21, and 0.20 eV for $1L$, $2L$, $3L$, and bulk MoS_2, respectively). The value for the bulk is in good agreement with that reported in Ref. [36]. Figure 3(b) shows that the damping constant γ of the A exciton increases significantly with a decreasing number of layers. The γ constant of the B exciton increases slightly with a decreasing number of layers and the C exciton γ is practically constant. These results explain why the REP of the A_{1g} mode is smeared out in the case of few-layer MoS_2 and why the A exciton REP is weaker than the B exciton REP [14].

According to the theoretical calculation by Qiu *et al.* [1], the broad band observed by optical absorption has the contribution of different excitonic transitions. By symmetry arguments based on group theory, we show that the in-plane E^1_{2g} mode couples with the C exciton. The difference between the sharp width of the resonance Raman profile and the broad band observed by other experimental techniques [37–40], is due to the fact that, differently from Raman scattering, these techniques do not involve exciton-phonon interactions. Therefore our results allow distinction of the contribution of the C exciton from all other excitonic states.

In conclusion, we have presented a resonance Raman study of 2D and bulk MoS_2 using many different laser lines in the range of 1.85 to 2.81 eV, that allowed us to obtain the resonance Raman profile of the first order A_{1g} and E^1_{2g} phonon modes. We have shown that the A_{1g} phonon mode is enhanced by the A and B excitons, but the enhancement decreases with a decreasing number of layers, due to the dependence of the lifetime of the intermediate excitonic states on the number of layers. We observed for the first time that the E^1_{2g} phonon mode is strongly enhanced around 2.7 eV, in a region of the optical spectrum that exhibits a broad band associated with a diversity of excitons [1]. A group theory analysis shows that the high energy C exciton is responsible for the enhancement of the E^1_{2g} phonon mode, due to the symmetry-dependent exciton-phonon interaction in MoS_2.

This work was supported by the Instituto Nacional de Ciência e Tecnologia (INCT) em Nanomateriais de Carbono (Federative Republic of Brazil), Coordenação de Aperfeiçoamento de Pessoal de Nível Superior (CAPES, Federative Republic of Brazil), Conselho Nacional de Desenvolvimento Científico e Tecnológico (CNPq, Federative Republic of Brazil) and Fundação de Amparo à Pesquisa do Estado de Minas Gerais (FAPEMIG, Federative Republic of Brazil). The authors thank Professor Tony Heinz, Professor James Hone, Dr. Flavio Plentz, and Dr. Changgun Lee for sample preparation.

*brunorc@fisica.ufmg.br
†mpimenta@fisica.ufmg.br

[1] D. Y. Qiu, F. H. da Jornada, and S. G. Louie, Phys. Rev. Lett. **111**, 216805 (2013).
[2] X. Xu, W. Yao, D. Xiao, and T. F. Heinz, Nat. Phys. **10**, 343 (2014).

[3] K. F. Mak, K. L. McGill, J. Park, and P. L. McEuen, Science **344**, 1489 (2014).
[4] P. Y. Yu and M. Cardona, *Fundamentals of Semiconductors* (Springer-Verlag, Berlin, 1982).
[5] T. Sekine, T. Nakashizu, M. Izumi, K. Toyoda, K. Uchinokura, and E. Matsuura, J. Phys. Soc. Jpn. Suppl. A **49**, 551 (1980).
[6] C. Sourisseau, F. Cruege, M. Fouassier, and M. Alba, Chem. Phys. **150**, 281 (1991).
[7] G. L. Frey, R. Tenne, M. J. Matthews, M. S. Dresselhaus, and G. Dresselhaus, Phys. Rev. B **60**, 2883 (1999).
[8] K. Golasa, M. Grzeszczyk, P. Leszczyński, C. Faugeras, A. A. L. Nicolet, A. Wysmolek, M. Potemski, and A. Babiński, Appl. Phys. Lett. **104**, 092106 (2014).
[9] J.-H. Fan, P. Gao, A.-M. Zhang, B.-R. Zhu, H.-L. Zeng, X.-D. Cui, R. He, and Q.-M. Zhang, J. Appl. Phys. **115**, 053527 (2014).
[10] H. Terrones *et al.*, Sci. Rep. **4**, 4215 (2014).
[11] M. A. Pimenta, E. del Corro, B. R. Carvalho, C. Fantini, and L. M. Malard, Acc. Chem. Res. **48**, 41 (2015).
[12] L. Sun, J. Yan, D. Zhan, L. Liu, H. Hu, H. Li, B. K. Tay, J.-L. Kuo, C.-C. Huang, D. W. Hewak, P. S. Lee, and Z. X. Shen, Phys. Rev. Lett. **111**, 126801 (2013).
[13] E. del Corro, H. Terrones, A. Elias, C. Fantini, S. Feng, M. A. Nguyen, T. E. Mallouk, M. Terrones, and M. A. Pimenta, ACS Nano **8**, 9629 (2014).
[14] N. Scheuschner, O. Ochedowski, M. Schleberger, and J. Maultzsch, Phys. Status Solidi B **249**, 2644 (2012).
[15] H. Li, Q. Zhang, C. C. R. Yap, B. K. Tay, T. H. T. Edwin, A. Olivier, and D. Baillargeat, Adv. Funct. Mater. **22**, 1385 (2012).
[16] B. Chakraborty, A. Bera, D. V. S. Muthu, S. Bhowmick, U. V. Waghmare, and A. K. Sood, Phys. Rev. B **85**, 161403(R) (2012).
[17] See Supplemental Material at http://link.aps.org/supplemental/10.1103/PhysRevLett.114.136403 for experimental details, the enhancement factor due to optical interference in the SiO_2 layer, crystalline structure, Raman-active modes, and the polarization analysis on the MoS_2 sample, which include Refs. [18–25]
[18] C. Lee, H. Yan, L. E. Brus, T. F. Heinz, J. Hone, and S. Ryu, ACS Nano **4**, 2695 (2010).
[19] S.-L. Li, H. Miyazaki, H. Song, H. Kuramochi, S. Nakaharai, and K. Tsukagoshi, ACS Nano **6**, 7381 (2012).
[20] D. Yoon, H. Moon, Y. W. Son, J. S. Choi, B. H. Park, Y. H. Cha, Y. D. Kim, and H. Cheong, Phys. Rev. B **80**, 125422 (2009).
[21] P. Klar, E. Lidorikis, A. Eckmann, I. A. Verzhbitskiy, A. C. Ferrari, and C. Casiraghi, Phys. Rev. B **87**, 205435 (2013).
[22] J. M. Chen and C. S. Wang, Solid State Commun. **14**, 857 (1974).
[23] T. Sekine, T. Nakashizu, K. Toyoda, K. Uchinokura, and E. Matsuura, Solid State Commun. **35**, 371 (1980).
[24] A. M. Stacy and D. T. Hodul, J. Phys. Chem. Solids **46**, 405 (1985).
[25] R. Loudon, Adv. Phys. **13**, 423 (1964).
[26] J. A. Wilson and A. D. Yoffe, Adv. Phys. **18**, 193 (1969).
[27] A. Molina-Sánchez and L. Wirtz, Phys. Rev. B **84**, 155413 (2011).
[28] J. B. Renucci, R. N. Tyte, and M. Cardona, Phys. Rev. B **11**, 3885 (1975).
[29] K. F. Mak, C. Lee, J. Hone, J. Shan, and T. F. Heinz, Phys. Rev. Lett. **105**, 136805 (2010).
[30] A. R. Beal and H. P. Hughes, J. Phys. C **12**, 881 (1979).
[31] R. A. Bromley, R. B. Murray, and A. D. Yofee, J. Phys. C **5**, 759 (1972).
[32] A. R. Beal, J. C. Knights, and W. Y. Liang, J. Phys. C **5**, 3540 (1972).
[33] W. Kauschke, V. Vorlicek, and M. Cardona, Phys. Rev. B **36**, 9129 (1987).
[34] W. Limmer, H. Leiderer, K. Jakob, W. Gebhardt, W. Kauschke, A. Cantarero, and C. Trallero-Giner, Phys. Rev. B **42**, 11325 (1990).
[35] M. Cardona and G. Güntherodt, *Light Scattering in Solids II* (Springer-Verlag, Berlin, 1982).
[36] R. Coehoorn, C. Haas, and R. A. de Groot, Phys. Rev. B **35**, 6203 (1987).
[37] A. Molina-Sánchez, D. Sangalli, K. Hummer, A. Marini, and L. Wirtz, Phys. Rev. B **88**, 045412 (2013).
[38] A. R. Klots, A. K. M. Newaz, B. Wang, D. Prasai, H. Krzyzanowska, J. Lin, D. Caudel, N. J. Ghimire, J. Yan, B. L. Ivanov, K. A. Velizhanin, A. Burger, D. G. Mandrus, N. H. Tolk, S. T. Pantelides, and K. I. Bolotin, Sci. Rep. **4**, 6608 (2014).
[39] J. Mertens, Y. Shi, A. Molina-Sánchez, L. Wirtz, H. Y. Yang, and J. J. Baumberg, Appl. Phys. Lett. **104**, 191105 (2014).
[40] H.-L. Liu, C.-C. Shen, S.-H. Su, C.-L. Hsu, M.-Y. Li, and L.-J. Li, Appl. Phys. Lett. **105**, 201905 (2014).